STUDY OF MESOSYSTEMS ASSOCIATED WITH STATIONARY RADAR ECHOES [1]

By Tetsuya Fujita

The University of Chicago

(Original manuscript received 26 March 1958)

ABSTRACT

Mesosystems associated with stationary radar echoes were analyzed. Five of them occurred on 20 July 1956 over the area of the U. S. Weather Bureau's Severe Local Storms Network, and they grew to 300–400 mi in diameter. Divergence and vorticity at each 1000-ft level inside a composite mesosystem were computed up to 5000 ft. It is found that the wind field is rotational up to 3000 ft where it becomes irrotational. Appreciable divergence reaching over 100×10^{-5} per sec on the ground decreases linearly to 30×10^{-5} per sec at the 5000-ft level. Computed vertical velocity inside the mesosystems was about 1 ft per sec at 1000 ft, reaching 3 ft per sec at the 5000-ft level. A small system of 13 August 1947 over the Thunderstorm-Project area was also studied; it was only 20 mi in diameter. Comparison of the characteristics of these systems indicated that the systems, large and small, may be produced by similar processes.

1. Introduction

Meteorological disturbances in medium scale, which we now call "mesoscale," are studied by those who are particularly interested in severe storms. This is a scale which might be overlooked in our daily synoptic analysis; however, if we try to take a close look at some of these mesoscale systems, it will be found that they are associated with extremely large values of time and space change in meteorological elements such as pressure, temperature, wind velocity, *etc.*

Suckstorf [1] postulated that the pressure rise beneath the convective clouds is a result of the rush of cold air descending from the precipitation clouds, and he established a model of cold-air overflow. Quantitative measurements of updrafts and downdrafts accompanied by thunderstorms were done by the Thunderstorm Project [2], and the source of the cold air reaching the ground was found to be downdrafts reaching up to 60 ft per sec.

The problem of hurricane formation was attacked by Bergeron [3] who emphasized the potential importance of the small highs at low levels within the area of rain cooling.

In the midwest, pressure systems appear in a much larger scale than can be found beneath a thunderstorm cloud. Following the close study of these systems, the question arose as to what extent we can assume that they resulted from thunderstorm activity. Tepper [4] pointed out the important fact that the pressure jump at the leading edge of the system is not always accompanied by thunderstorms or a temperature drop. It is known that the time difference between pressure jump and temperature drop is sometimes several hours.

A sufficient number of case studies has not been done, so far, to permit a reasonable classification of mesoscale systems. Until now, they have been variously designated, and in the literature we find the following examples: "rain induced high" by Oliver Holzworth [5]; "elevation, depression and combination type wave," Williams [6]; "pressure jump," Tepper [4]; "thunderstorm high," Byers [7]; "bubble squall line and micro-anticyclone," Fawbush and Miller [8]; "wake depression," Fujita [9]; "mesohigh and mesolow," Stout, Blackmer, Holleyman and Gibson [10]; "tornado cyclone," Brooks [11]; and others.

The importance of mesoanalysis was emphasized by the joint authors, Fujita, Newstein, and Tepper [12] in their representation of complicated mesoscale features in color.

In the present article, a small high-pressure system associated with several thunderstorm cells, and large mesoscale systems 200–400 mi in horizontal dimensions, were studied. The former occurred over the Thunderstorm Project Network, Ohio, and the latter ones occurred over the Severe Local Sotrm Microbarograph Network, Texas and Oklahoma. Keymaps of these two networks appear in fig. 1.

2. Mesoscale high of 20 July 1956

The mesoanalysis area, 500 × 600 nautical miles in size, covers the states of Texas, Oklahoma, Louisiana, and Arkansas. Weather Bureau radars, equipped with 16-mm cameras, were in operation at Oklahoma City, Oklahoma, at Abilene, San Angelo, San Antonio, and Austin in Texas, and at Lake Charles and Baton

[1] The research reported in this paper has been sponsored by the United States Weather Bureau, under contract Cwb 9231.

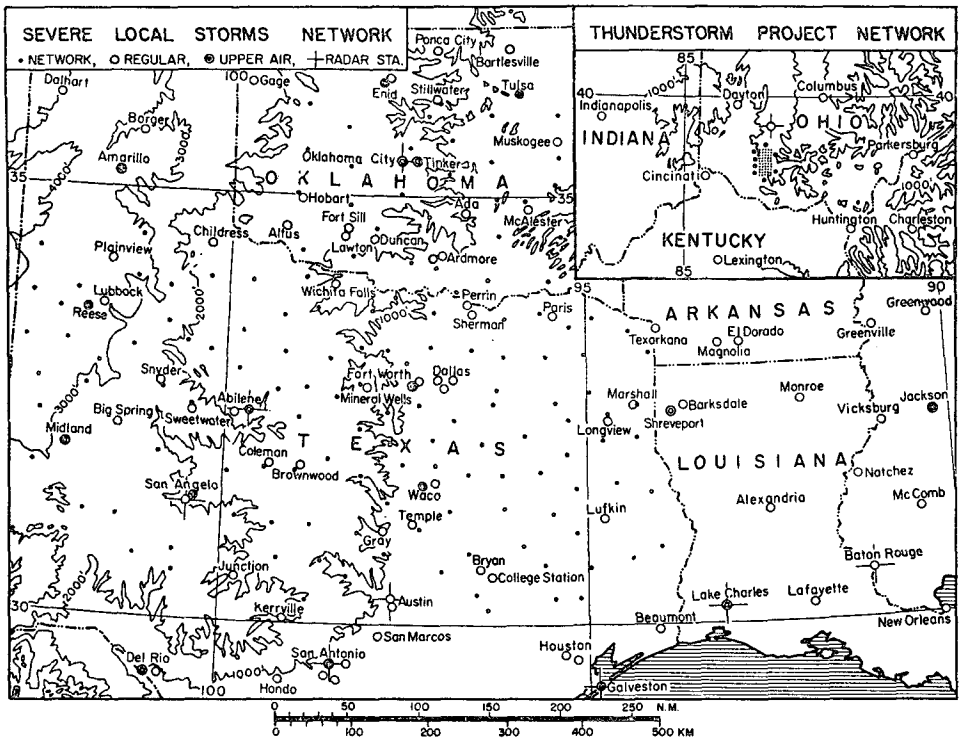

FIG. 1. The area of the Thunderstorm Project, Ohio, and the Severe Local Storm Microbarograph Networks.

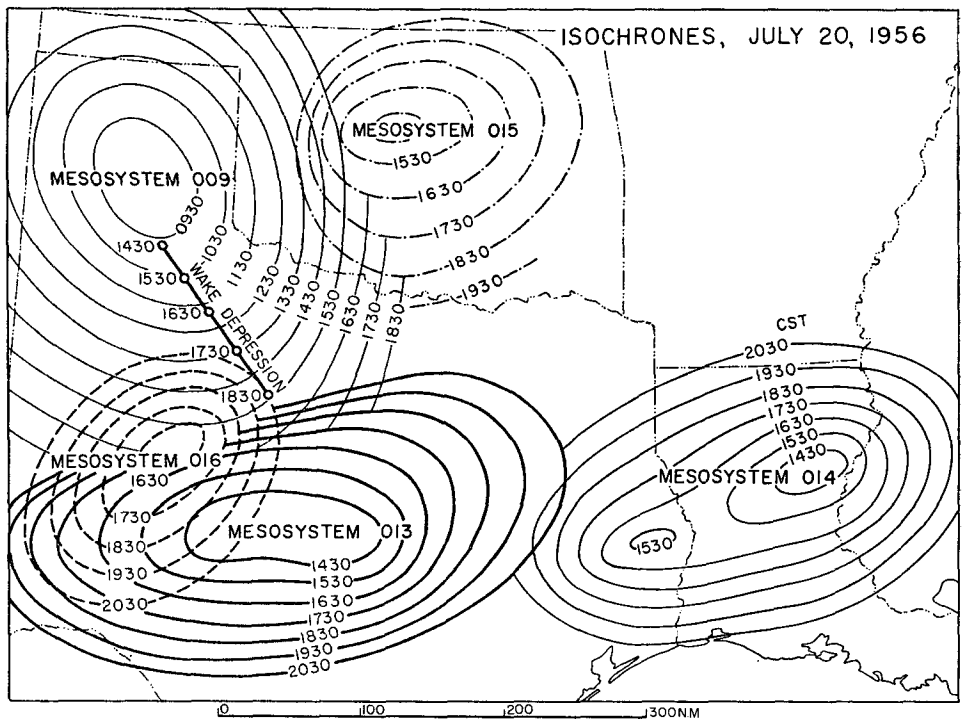

FIG. 2. Isochrones of five systems on 20 July 1956. The systems are numbered by the day and the hour of their first appearance in the mesoanalysis charts. Mesosystem 009 denotes, for instance, that this system appeared on the 20th at 0900 CST.

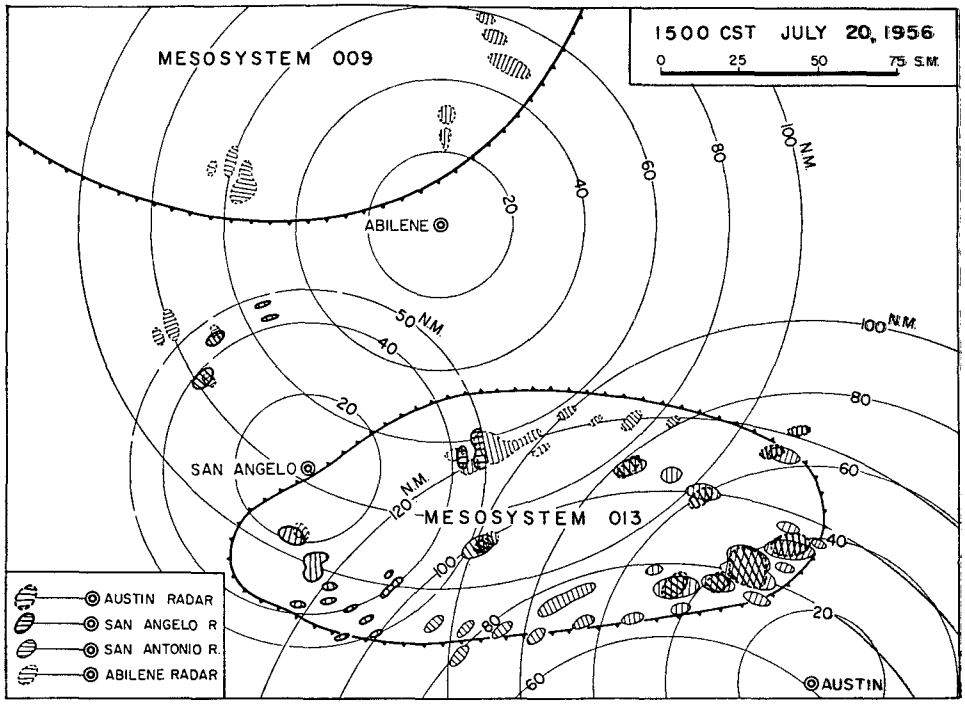

FIG. 3. Composite radar-echo chart made by organizing radar pictures from five stations in Texas. The shading represents the direction of beams of one or more radars which picked up a particular echo.

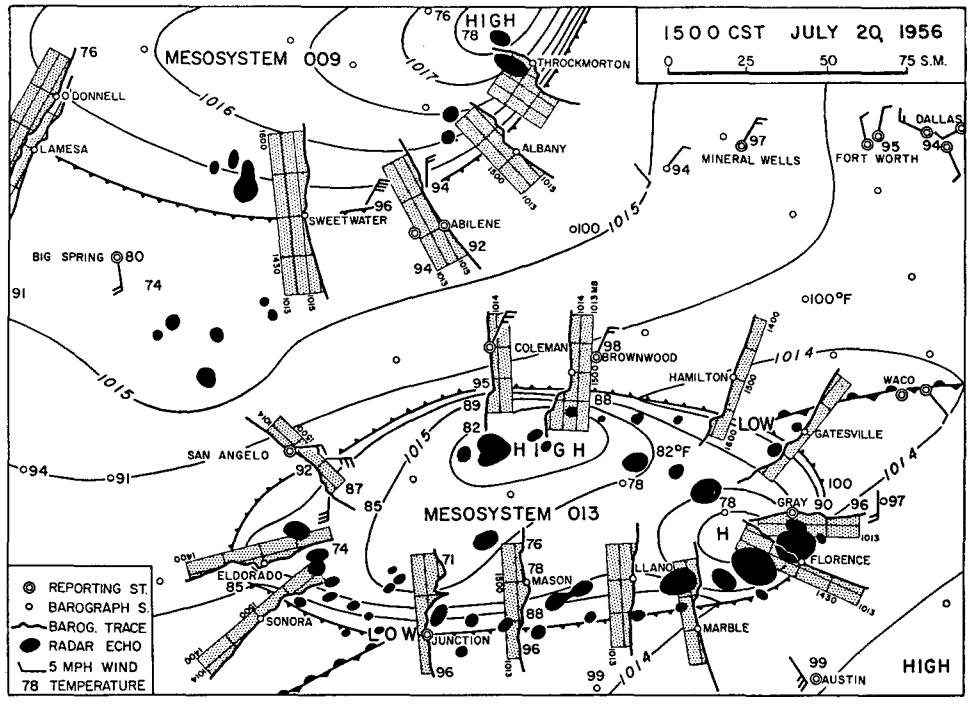

FIG. 4. Mesoanalysis of the surface chart covering the area of fig. 3. Time sections of station pressures are converted into space distribution along vectors perpendicular to each system boundary. Stippled areas denote the sea-level pressure above 1013 mb.

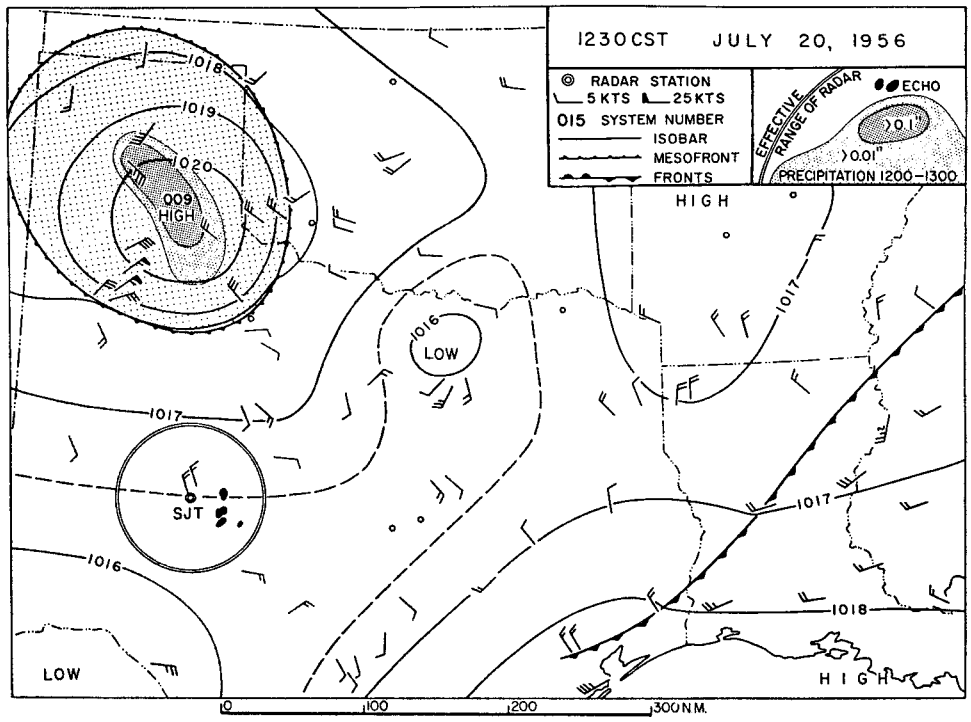

FIG. 5. Mesoanalysis chart at 1230 CST 20 July 1956.

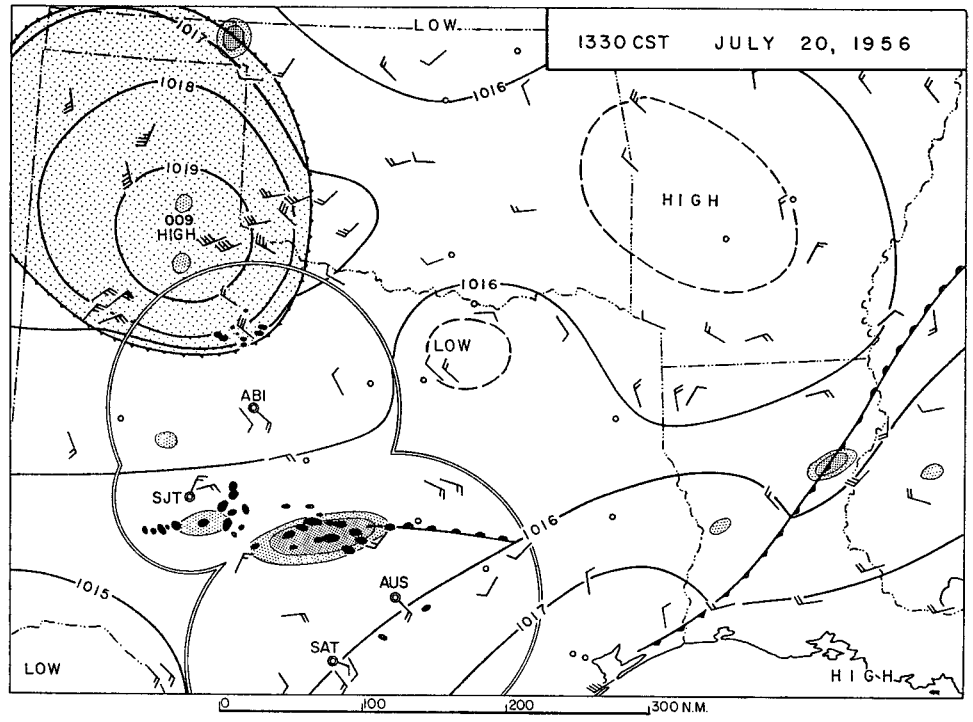

FIG. 6. Mesoanalysis chart at 1330 CST 20 July 1956.

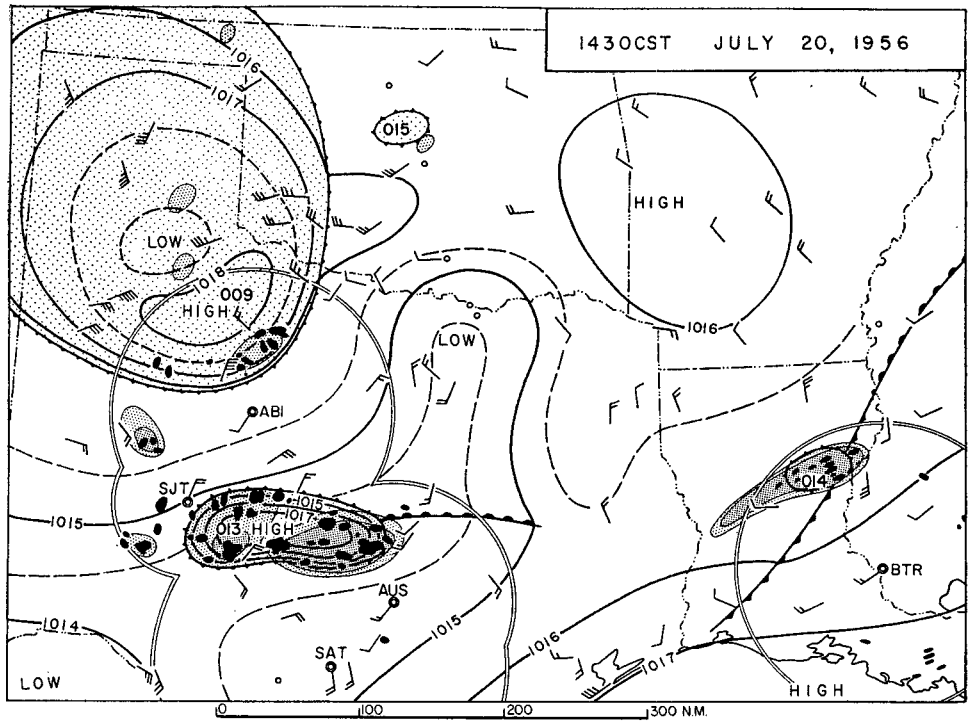

FIG. 7. Mesoanalysis chart at 1430 CST 20 July 1956.

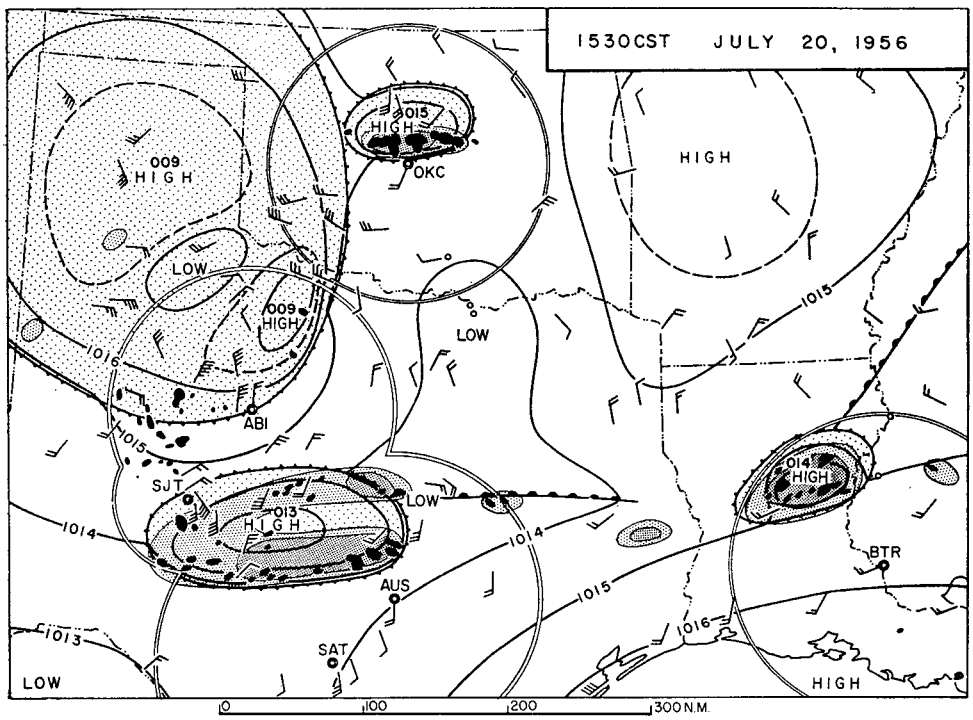

FIG. 8. Mesoanalysis chart at 1530 CST 20 July 1956.

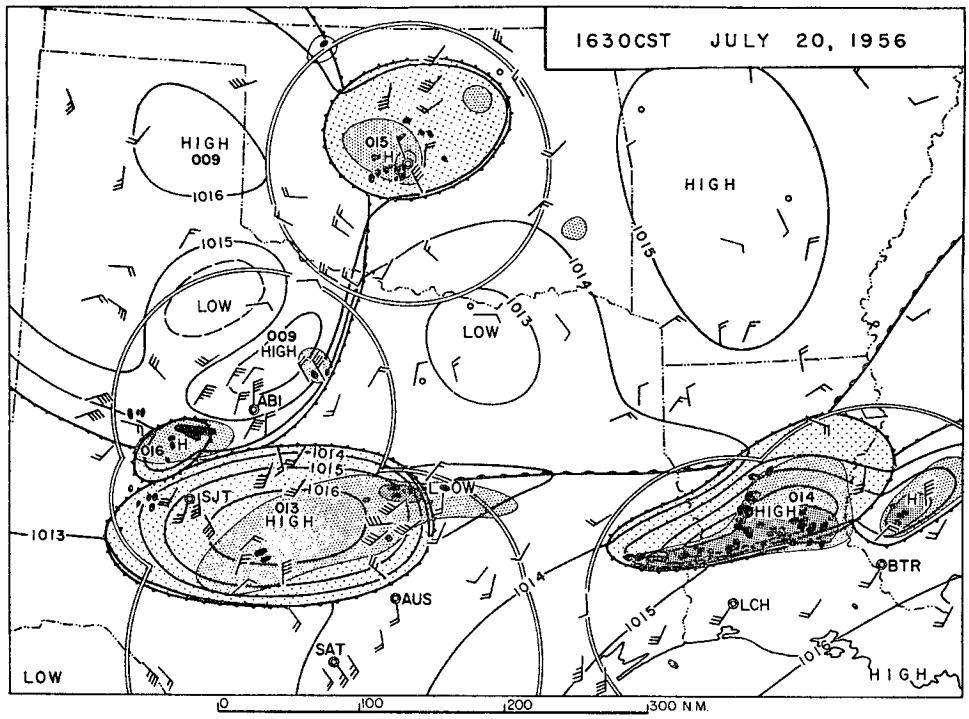

FIG. 9. Mesoanalysis chart at 1630 CST 20 July 1956.

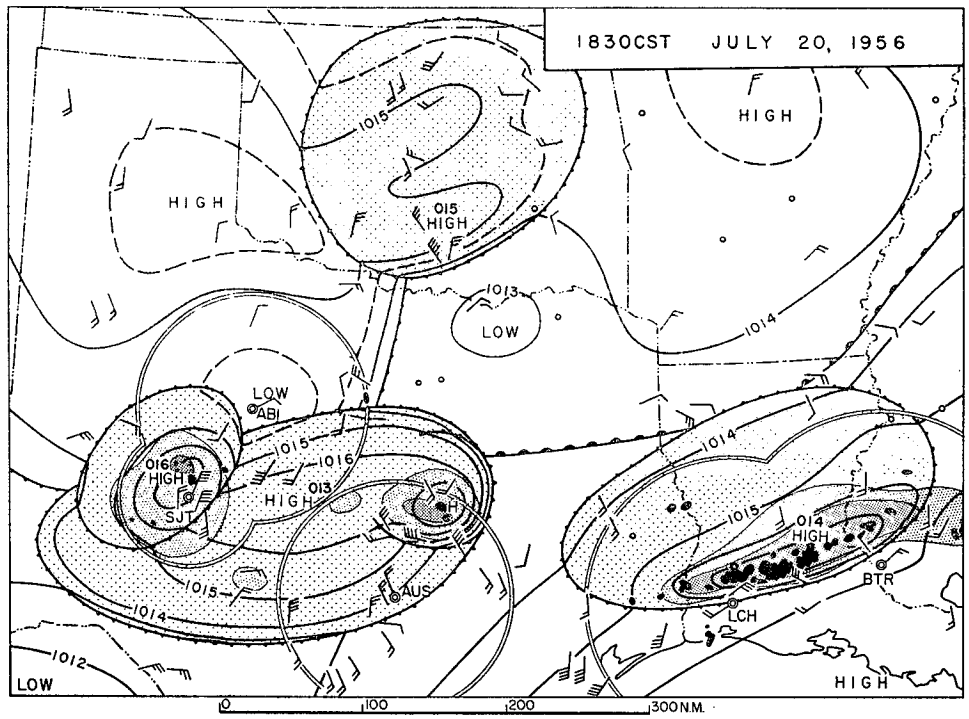

FIG. 10. Mesoanalysis chart at 1830 CST 20 July 1956.

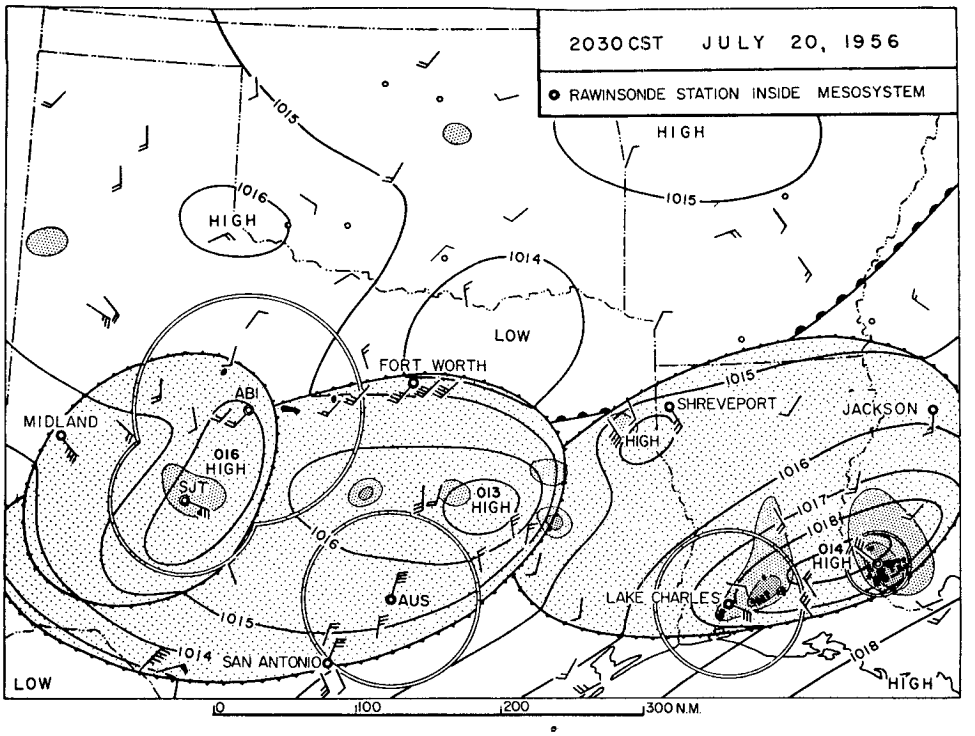

FIG. 11. Mesoanalysis chart at 2030 CST 20 July 1956. Rawinsonde observations were made at the six stations located inside the three mesoscale high pressure systems at 2100 CST. All three systems were in their dissipating stage, characterized by scattered showers.

Rouge in Louisiana. A preliminary analysis of echoes over the analysis area indicated that their movement was very slow, only 0–5 mph south-southeastward. Therefore, the time change in echoes took place mainly due to formation and dissipation.

Fig. 2 reveals the isochrones of systems 009, 013, 014, 015, and 016 which appeared in the hourly charts at 0900, 1300, 1400, 1500, and 1600 CST, respectively. It is found that the isochrones expanded with time into all directions. This phenomenon is not seen in the case of a system associated with rapidly moving echoes.

An example of construction of a radar-echo chart is given in fig. 3. A brief examination of the range marks on radar films showed that they were not true circles and, moreover, were not equidistant. To correct these distortions, the echoes of the original pictures were first transcribed on polar coordinates having the scale of the base chart. The echoes were again transcribed on the composite chart and shaded by the direction of beams of each radar by which they had been detected.

It is of interest to recognize that the location of a particular echo did not vary much when fixed by two or more radars; the maximum difference was only a few miles. If a composite chart was made in the region of vertical shear, the tilt of echo axes would result in a considerable change in the location of a particular echo detected from different distances. The difference in gain among radar pictures presents a difficult problem in organizing composite echo patterns.

Fig. 4 represents the mesoanalysis of the surface chart having the same scale as the composite echo chart. The conversion of time sections into space sections was made along vectors perpendicular to the isochrone of a system boundary. The final analysis was done, therefore, by turning the chart around 360 degrees.

The first hourly chart for 1230 CST appears in fig. 5. The echoes within the effective range of radars in operation are shown in black, and the surface precipitation in a one-hour period covering 30 min before and after the map time is contoured by 0.01- and 0.1-in isohyets. The only mesoscale disturbance seen in the chart at this time is System 009, which was formed at 0900 CST on the 20th. Precipitation cells inside this system were not detected by radar; however, the hourly rainfall reveals the existence of surface rain near the center of the system.

Fig. 6 gives the situation at 1330 CST. System 009 which is now in its dissipating stage is characterized by scattered small showers near its southeastern boundary. An appreciable wind surge is noticed all around the boundary at which the pressure rises slowly or rapidly, as much as 1–2 mb. The echoes

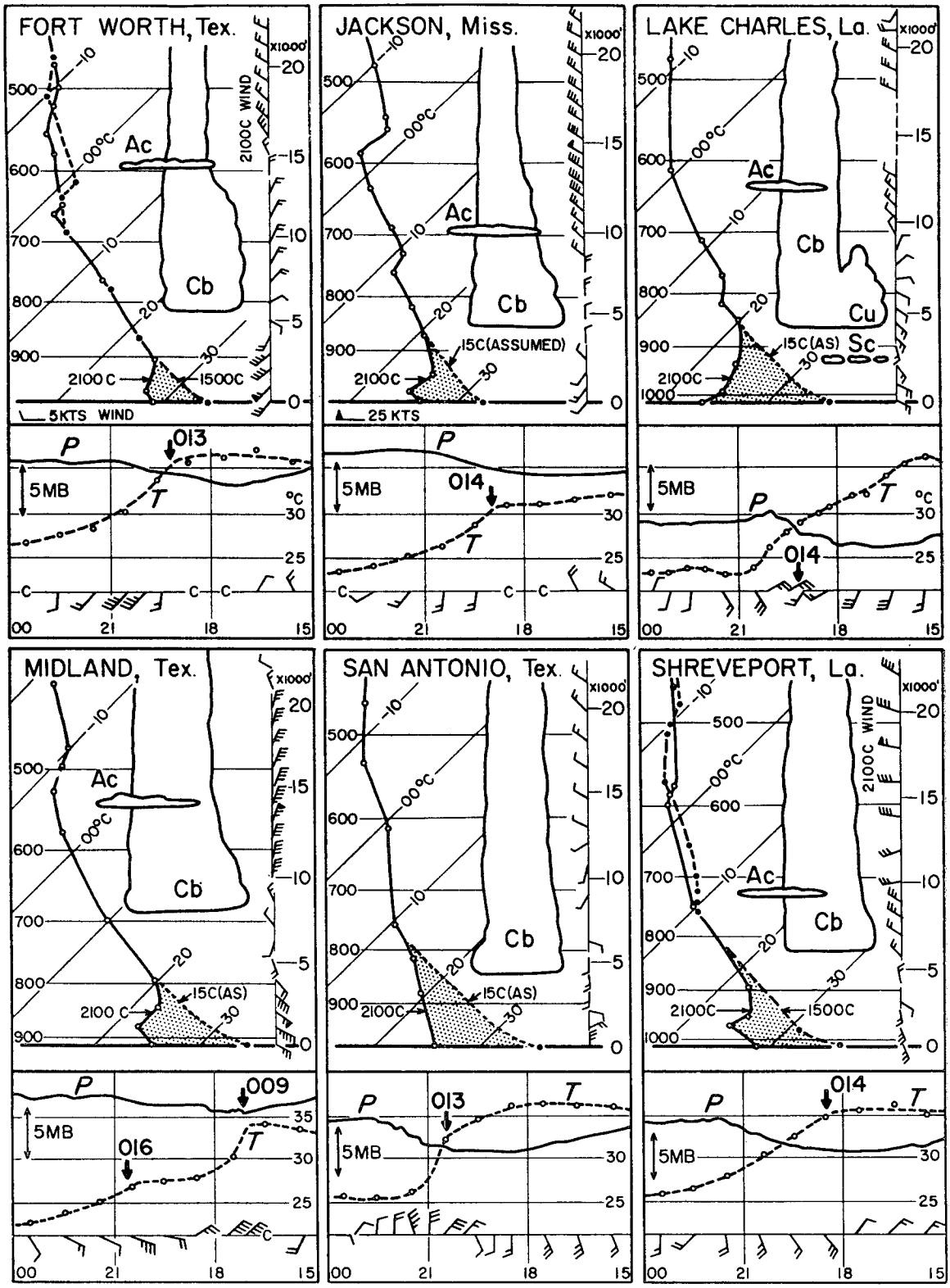

FIG. 12. Temperature and winds aloft from the six rawinsonde stations indicated in fig. 11. The 1500 CST ascent is available for Fort Worth, Tex., and Shreveport, Louisiana.

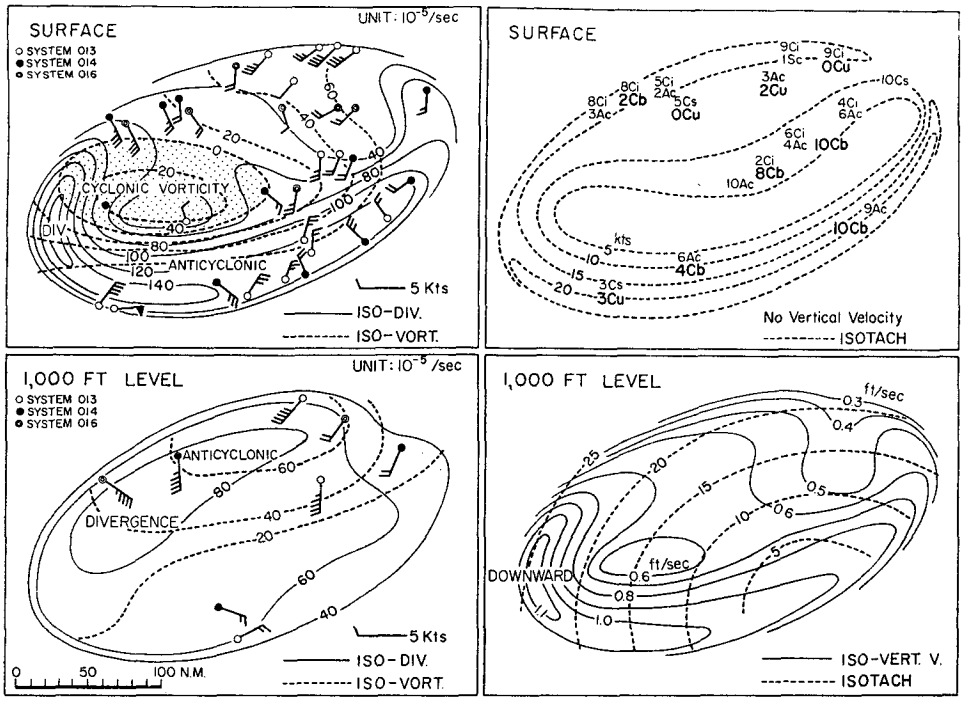

FIG. 13. Divergence, vorticity, isotach, and vertical velocity analysis of the composite wind field of systems 013, 014, and 016 at 2030 CST (surface) and 2100 CST (1,000 ft) 20 July 1956.

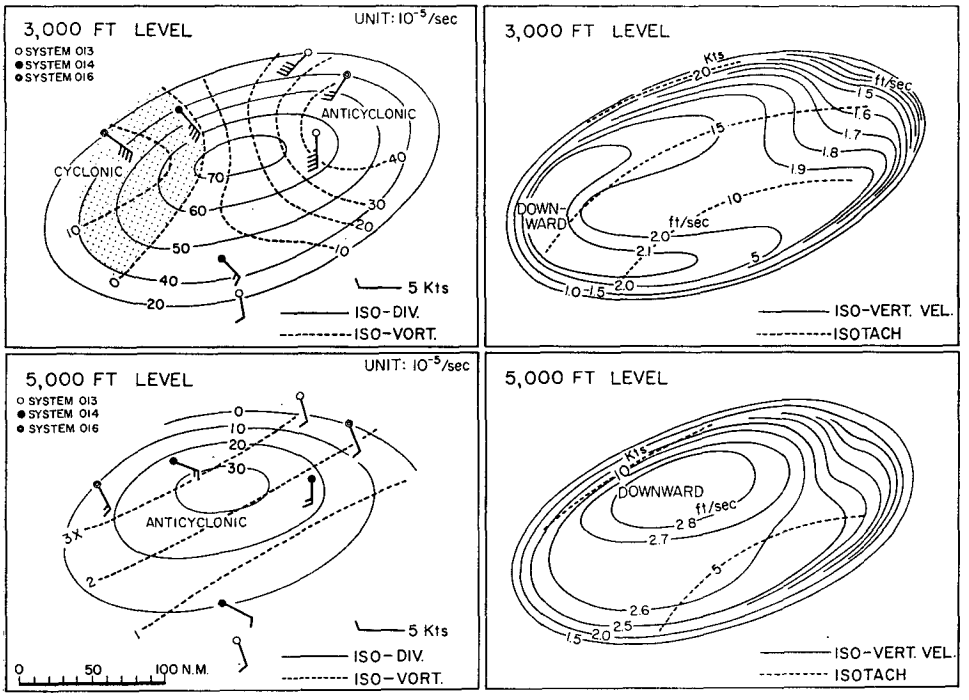

FIG. 14. Divergence, vorticity, isotach, and vertical velocity analysis of the composite wind field of systems 013, 014, and 016 at 2100 CST 20 July 1956.

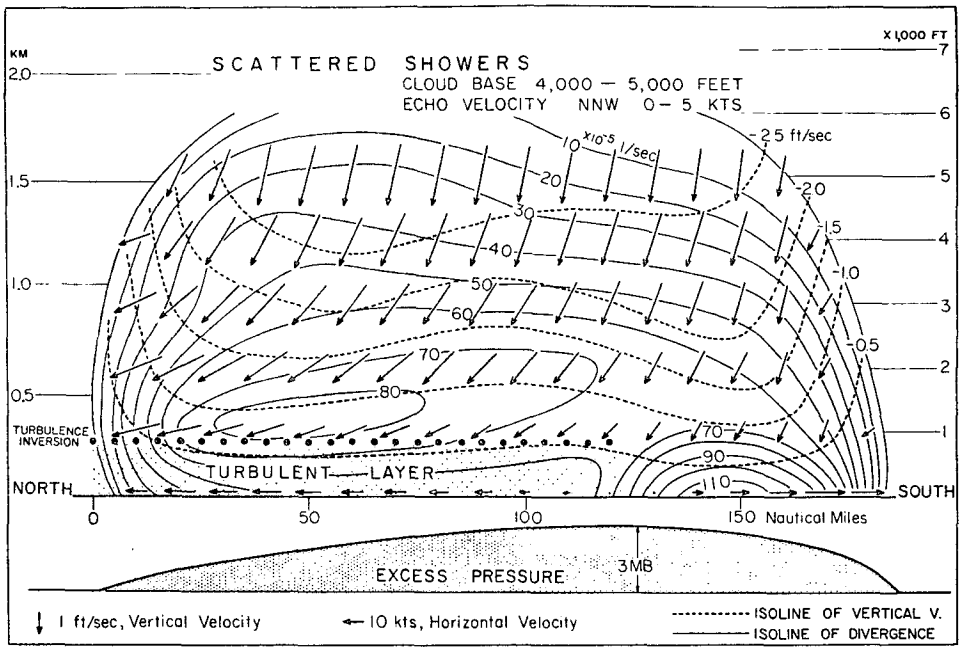

FIG. 15. Showing the north-south vertical cross-section of the composite system appearing in figs. 13 and 14. Maximum divergences are seen above the earth and the inversion surfaces which force the descending air to spread out.

between San Angelo and Austin increased in number and grew in size. A couple of microbarograph stations beneath the echoes indicated humps about this time, but they have not been organized for analysis in the scale of this chart. Scattered showers were seen in the frontal zone over Louisiana and Mississippi.

As seen in fig. 7, Mesosystem 013 was organized at 1430 CST. This system contained 32 echoes, 5 mi in average diameter. We notice that the echo activity is significant near the edge of the system. This characteristic is clearly seen in the chart for 1500 CST, fig. 4. System 014 is now developing in Louisiana, and its major part is covered by the effective range of the Baton Rouge radar. A striking feature, a mesoscale low, appeared inside System 009. The amount of pressure drop associated with the low is only half a millibar, but it was recorded at many stations in the area of low development.

System 013 at 1530 CST (fig. 8), was characterized by thunderstorm activity along the system boundary. The mesoscale low inside the system deepened with the intensification of the high. A heavy solid-line echo appeared in the area, 50 mi east of the boundary of System 009, where a new mesohigh started developing.

Remarkable echoes in line were pictured by the Lake Charles and Baton Rouge radars; they appear in the composite echo chart (fig. 9). The associated System 014 has now grown into a regular-size mesosystem. By this time, System 013 has reached its dissipating stage with little activity and some drizzle within its boundaries. The solid-line echoes north of Oklahoma City have disintegrated into scattered echoes.

Fig. 10 reveals that precipitation no longer existed in System 015 at 1830 CST. However, the boundary of the system was still expanding. The new System 016 started developing in the area covered by Systems 009 and 013.

The last hourly chart for 2030 CST (fig. 11) is prepared in order to show the situation when the 2100 CST upper-air observations were made. We notice that six rawinsonde stations were then located inside three mesosystems in their dissipating stage.

3. Vertical structure of composite mesohigh

An attempt was made to investigate the vertical structure of the mesosystems by careful use of the six ascents made at 2100 CST. Fig. 12 shows the temperature and winds aloft of these ascents. Time changes in pressure, temperature, and wind appear in the lower section of each diagram. The arrows in the chart indicate the time at which each system reached the station.

Only two stations, Fort Worth and Shreveport, made upper-air observations at 1500 CST. The temperature of these ascents indicates fairly well the condition before the stations were affected by the

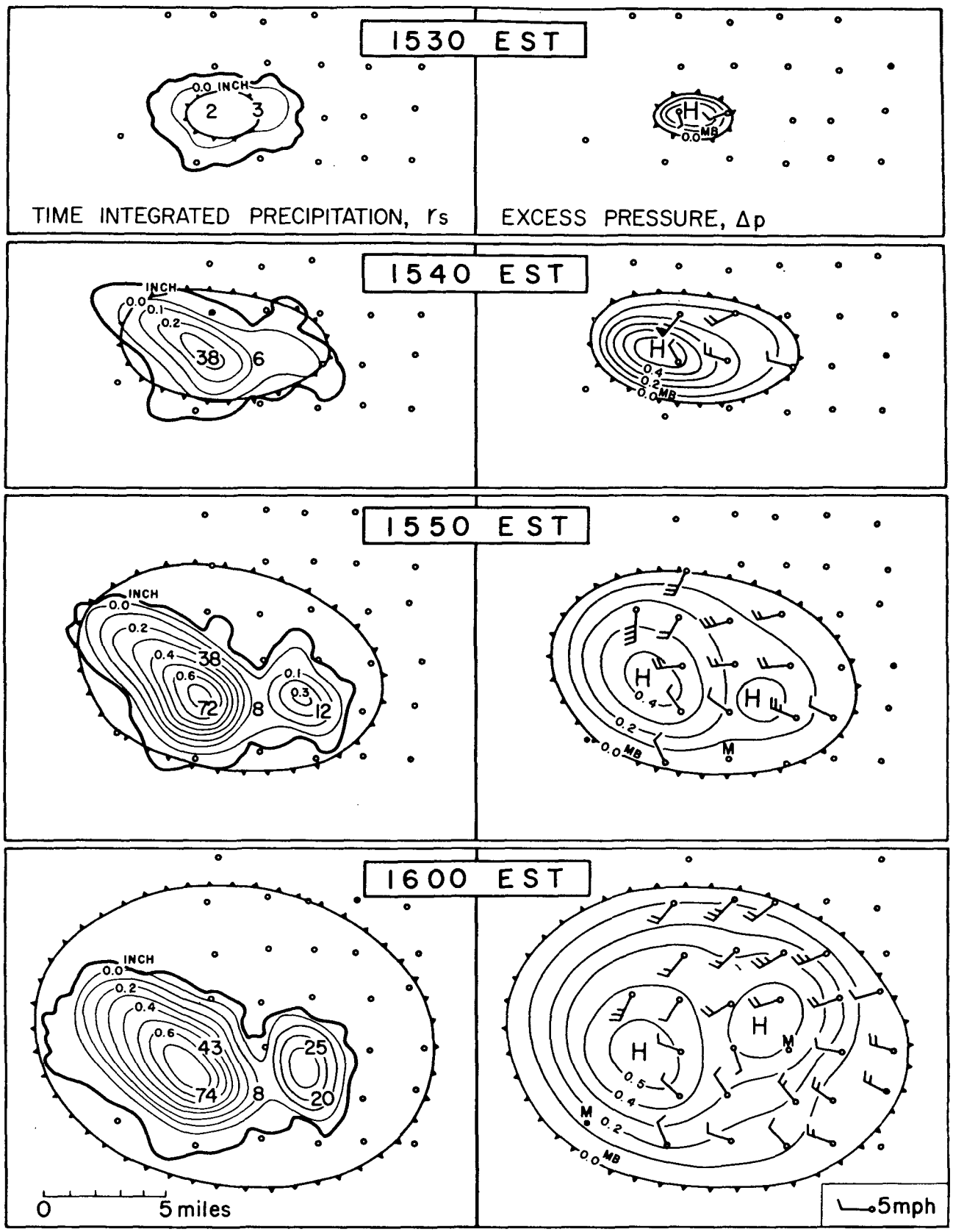

FIG. 16. The time-integrated echo boundary and precipitation amount of a cellular thunderstorm high on 13 August 1947 over the Ohio Network of the Thunderstorm Project. The Project stations are indicated by small circles. The excess pressure field inside the boundary of the system is analyzed with the help of the surface winds pushing outward from the activity centers.

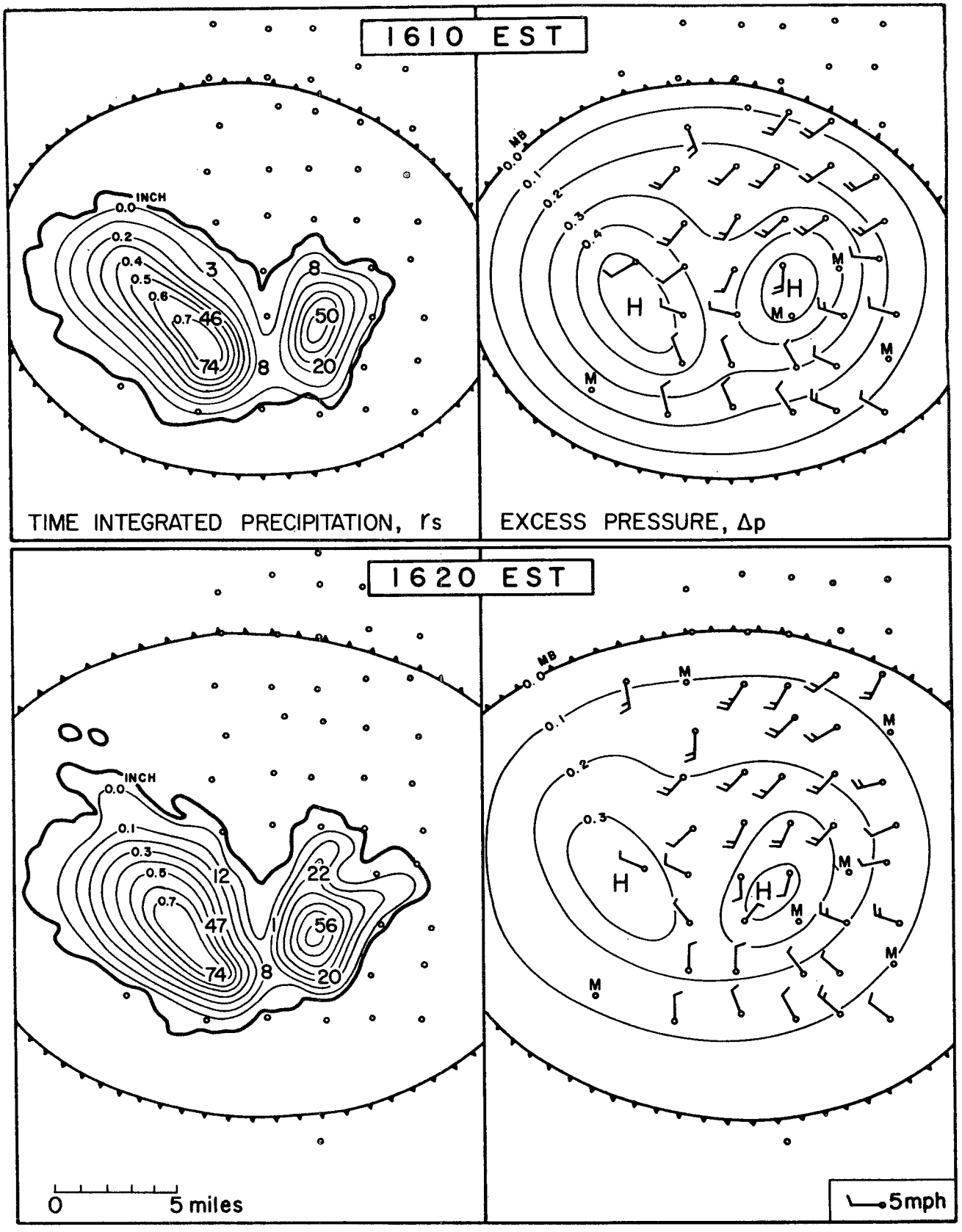

FIG. 17. The last feature of the cellular thunderstorm high of 13 August 1947 over the Ohio Network of the Thunderstorm Project.

mesosystems. In order to estimate the temperature drop due to the mesosystems, vertical distributions of temperature for 1500 CST at Jackson, Lake Charles, Midland, and San Antonio are assumed with the help of the surface temperature and the expected dry-adiabatic lapse rate. The stippled areas thus obtained represent the amount of low-level cooling associated with the systems.

Surface and upper-air composite charts of Mesosystems 013, 014 and 016 were made by enlarging or reducing each system to average dimensions. Then the winds observed in different systems were finally plotted in one composite system of mean shape. The distribution of surface winds given in fig. 13 reveals that the winds in the composite chart are sufficiently organized to permit the computation of divergence and vorticity. Upper-air composite charts were made at each 1000-ft level up to 5000 ft, and the analyses of wind fields were done using the author's method [9]. The results appear in figs. 13 and 14.

Very large divergence values on the ground, up to 160×10^{-5} per sec, are noticed in the area of relatively large convective activity near the sourthern edge of the composite system. In the northern part of the system, however, the divergence is rather small being 50×10^{-5} per sec. Such a distribution no longer exists at the 1000-ft level, and the maximum appears near the northern edge.

The vertical-wind velocity field can be computed by superposing the divergence fields, layer upon layer. Let D_0, D_1, D_2, $\cdots$, and w_0, w_1, w_2, $\cdots$, be the divergence and the vertical velocity at the surface, 1000 and 2000 ft above the surface, respectively. The assumptions of linear change in divergence between each 1000-ft layer and of incompressible atmosphere permit us to write:

$$-w_1 = (\tfrac{1}{2}D_0 + \tfrac{1}{2}D_1) \times 1000$$
$$-w_2 = (\tfrac{1}{2}D_0 + D_1 + \tfrac{1}{2}D_2) \times 1000$$
$$-w_3 = (\tfrac{1}{2}D_0 + D_1 + D_2 + \tfrac{1}{2}D_3) \times 1000$$
$$-w_4 = \cdots\cdots\cdots\cdots.$$

The results of computations are presented to the right of the divergence charts. It is noticed that the vertical velocity near the top of the system reached as high as -2.8 ft/sec.

Vorticity was also computed for each 1000-ft level. It was found that the surface-wind field was characterized by an area of cyclonic vorticity surrounded by an area of anticyclonic vorticity. The ratio of vorticity to divergence at the surface is only 0.5, about 1/20 of the ratio seen in regular synoptic scale. This ratio becomes much smaller as the height increases: only 0.1 at the high levels of the systems. This indicates that the irrotational wind field was located on top of the rotational field.

A north-south cross section of the composite mesosystem through its center is presented in fig. 15. The resultant vectors of the vertical and horizontal velocities are represented by arrows. It is of extreme interest to find the maximum divergence existing near the ground in the southern portion of the system where the convective activity was still going on. In the northern area, however, maximum divergence existed above the turbulent layer, the top of which is indicated by large dots. This layer is characterized by the dry-adiabatic lapse rate beneath the inversion as seen in the 2100 CST ascents from Fort Worth, Jackson, Midland, and Shreveport. It is very reasonable to imagine that the top of the turbulent layer was acting like a solid boundary which forces the subsiding air to diverge before reaching the ground. This can be the reason for the existence of the large divergence above the turbulent inversion.

4. Cellular high over the Thunderstorm Project network

A cellular high of 13 August 1947 over the Ohio Network of the Thunderstorm Project was investigated. This high, associated with a relatively isolated storm with several cells, developed inside the warm sector, about 300 mi from the cold front. Scattered thunderstorm echoes existed all over the area covered by the 150-mi range of the Project radar.

Time integrated precipitation, r_s, and echo boundary appear in figs. 16 and 17. These figures also show the boundary and the excess pressure Δp of the high-pressure system beneath the storm. The excess pressure was obtained, in this case, from the barograph traces and the surface isobars by subtracting the undisturbed pressure. As seen in the figures, the boundary of the pressure system started developing directly under the precipitation cell at 1530 CST. The area of the system, much smaller than that of the echo, increased rapidly, and in 20 min the leading edge of the system spread out far from the area of the time integrated echo boundary.

Areal integrations,

$$R_s = \int_S Rs\, dS \quad \text{and} \quad \Delta M = \frac{1}{g}\Delta P = \frac{1}{g}\int_S \Delta p dS,$$

where S is the area covered by the system, were done at 10-min intervals. Here, Rs and ΔM will be called the total amount of surface rain and the total amount of excess mass of cold air, respectively. Fig. 18 reveals the relationship between these values. It is evident that the excess mass increased in proportion to the total amount of surface rain. This fact implies that the production of cold air is closely related to the surface rain; however, the cold air does not have to be produced by the rain reaching the ground.

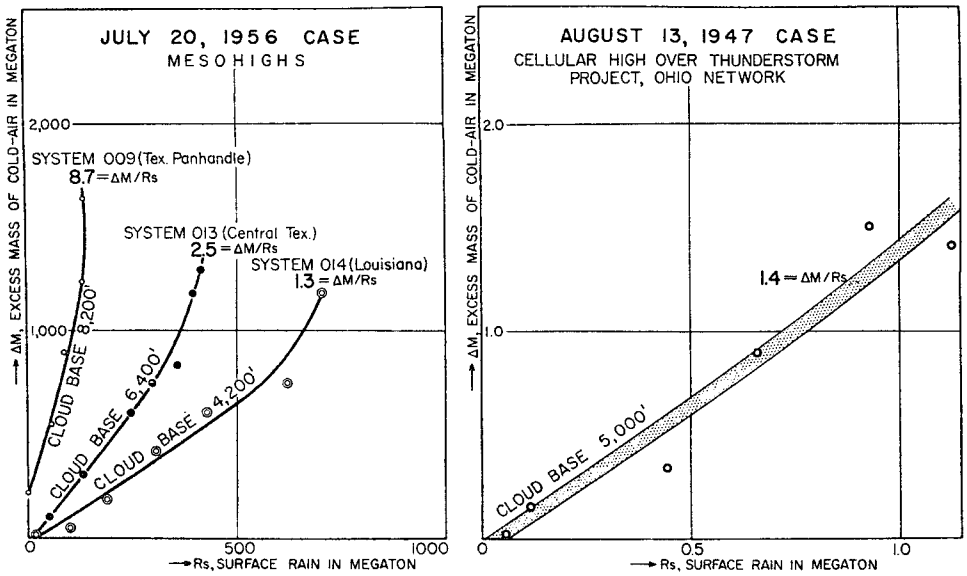

FIG. 18. Similarity of excess-mass increase in cellular and mesoscale highs. The ratio of the total amount of the excess mass to the surface rain, M/Rs, is found to be greatly affected by the height of the cloud base but not by the dimensions of the high pressure system.

The same integrations were carried out for the mesoscale highs of 20 July 1956. The ΔM-Rs chart, thus prepared, proves the existence of a relationship similar to the one found in the case of the cellular high. The rate of increase in ΔM is quite different in each case, however, and System 009 which developed over the Texas Panhandle shows an extremely large ratio of $\Delta M/Rs$; moreover, in this case, the associated cold air was present before the rain reached the ground.

A reasonable interpretation of these phenomena was undertaken by introducing a third parameter: the height of the convective cloud base above the ground. It was found that the higher the cloud base, the larger the ratio $\Delta M/Rs$. From this, one may assume that the cold-air production is closely related to the evaporation of raindrops as they fall under the cloud base toward the ground. Thus, cold air may already exist before the first rain drop hits the ground. Future study of virga and high-level thunderstorms, in connection with the height of the cloud base, will help solve this problem.

Another important fact is that the ratios, $\Delta M/Rs$, for the cellular and mesoscale systems, with similar height of cloud base, are almost identical: 1.3 and 1.4.

5. Conclusions

Careful analysis of the composite winds of three mesohighs in their dissipating stage revealed that the entire cold dome was a divergent field. However, the field was rotational up to 3000 ft where it became almost irrotational. At the top of the dome, about 5000 ft above the ground, vertical motion computed from divergence values was about 3 ft/sec. It seems reasonable to consider that the subsiding cold air gains its vorticity as it approaches the ground.

The study of high pressure systems, 20–400 mi in horizontal dimensions, reveals that the total amount of excess mass of cold air forming them increases in proportion to the total amount of surface rain. The ratio $\Delta M/Rs$ seems to increase appreciably with the height of the associated convective cloud base.

One of the mesoscale highs of 20 July 1956 and the cellular high of 13 August 1947, for which the heights of the cloud base were 4800 ft and 5000 ft above ground, respectively, were characterized by almost the same value of $\Delta M/Rs$, although the areal ratio of these systems was 1/400. The ratio $\Delta M/Rs$ does not seem to vary with the size of the systems.

It is not the purpose of this paper to present a mechanism of cold-air production by precipitation. However, the fact that $\Delta M/Rs$ is independent of the system's size and increases appreciably with the height of the convective cloud base will lead us to investigate the process of cold-air production by sub-cloud evaporation. Theoretical work on this problem is now in progress and detailed discussions will appear in a forthcoming article by the author.

Acknowledgments.—The author wishes to thank Dr. Horace R. Byers, Chairman of the Department of Meteorology, The University of Chicago, and Dr. Morris Tepper, U. S. Weather Bureau, for their kind help in completing this article.

REFERENCES

1. Suckstorff, G. A., 1935: Die Strömungsvorgänge in Instabilitätsschauern. *Z. Meteor.*, **52**, 449–452.
2. Byers, H. R., and R. R. Braham, Jr., 1949: *The thunderstorm.* Rep. of the Thunderstorm Project, 1946 and 1947, Govt. Printing Off., Washington, D. C.
3. Bergeron, T., 1954: Tropical hurricanes. *Quart. J. r. meteor. Soc.*, **80**, 131–164.
4. Tepper, M., 1950: A proposed mechanism of squall lines: the pressure jump. *J. Meteor.* **7**, 21–29.
5. Oliver, J. F., and G. C. Holzworth, 1953: Some effects of the evaporation of widespread precipitation on the production of fronts and on changes in frontal slopes and motions. *Mon. Wea. Rev.*, U. S. Wea. Bur. No. 81, 141–151.
6. Williams, D. T., 1953: Pressure wave observations in the Central Midwest, 1952. *Mon. Wea. Rev.*, U. S. Wea. Bur. No. 81, 278–289.
7. Byers, H. R., 1951: *Compendium of meteorology.* Amer. meteor. Soc., 681–693.
8. Fawbush, E. J., and R. C. Miller, 1954: The types of air mass in which North American tornadoes form. *Bull. Amer. meteor. Soc.*, **35**, 154–165.
9. Fujita, T., 1955: Results of detailed synoptic studies of squall lines. *Tellus*, **7**, 405–436.
10. Stout, G. E., R. H. Blackmer, Jr., J. B. Holleyman, and H. M. Gibson, 1957: *Mesometeorological analysis of atmospheric phenomena.* Quart. Tech. Rep. Nos. 1–10, Illinois State Water Survey.
11. Brooks, E. M., 1949: The tornado cyclone. *Weatherwise*, **2**, 32–33.
12. Fujita, T., H. Newstein, and M. Tepper, 1956: *Mesoanalysis: An important scale in the analysis of weather data.* U. S. Wea. Bur. Res. Pap. No. 39.